Pergamon

Bioorganic & Medicinal Chemistry 8 (2000) 1881–1891

BIOORGANIC & MEDICINAL CHEMISTRY

α-Ketoamides and α-Ketocarbonyls: Conformational Analysis and Development of All-Atom OPLS Force Field

Kalju Kahn and Thomas C. Bruice*

Department of Chemistry and Biochemistry, University of California-Santa Barbara, Santa Barbara, CA 93106, USA

Received 22 January 2000; accepted 29 March 2000

Abstract—The molecular structures and barriers for the internal rotation around the OC−CO single bond in four α-ketoamides and eight α-ketocarbonyls have been determined from the MP3/aug-cc-pVDZ and MP2/aug-cc-pVDZ calculations. α-Ketocarbonyls with non-bulky substituents adopt planar conformations with two carbonyl oxygens in s-*trans* arrangement. The s-*cis* conformation is significantly less stable due to the electrostatic repulsion between the two carbonyl groups. Primary and secondary α-ketoamides are planar when the substituent at the carbonyl carbon is hydrogen or methyl group but tertiary α-ketoamides adopt a conformation where the OC−CO unit is significantly bent. Based on current ab initio structural data, a set of OPLS−AA force field parameters has been derived. These parameters can be used for the modeling of a variety of α-ketoamide or α-ketocarbonyl containing drugs such as novel protease inhibitors or neuroregenerative polyketides.

Introduction

The α-ketoamide moiety (Scheme 1) is present in many pharmacologically interesting compounds, the most well-known examples being macrocyclic polyketides FK506 and rapamycin.[1–3] These polyketides have been thoroughly investigated due to their immunosuppresssive effect, and FK506 is currently approved for use by liver transplant recipients.[4] More recently, analogues of FK506 have received renewed attention because of their possible neuroregenerative effects.[4] It has been demonstrated that immunosuppressive and neuroregenerative effects of FK506 are due to the interaction of the drug with two different targets. The suppression of immune system requires binding of FK506 to the protein termed FKBP12 while the neuroregenerative effect is related to the interaction of FK506 with the protein FKBP52.[5–7] The naturally occurring polyketide FK506 has a higher affinity for the protein FKBP12, making it unsuitable as a neuroregenerative drug. Search for analogues of FK506 which are specific for FKBP52 has currently high priority, and to assist with this goal, we have recently developed computer-based methods for generating and screening virtual libraries of modified polyketides.[8,9] These methods depend critically on the quality of the underlying molecular mechanics force field, and the current paper focuses on the development and testing of OPLS−AA force field for α-ketoamide-containing compounds.

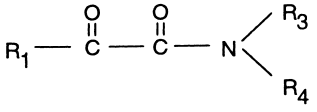

Scheme 1.

Besides immunosuppressive polyketides, the α-ketoamide group is also an important constituent of many potent protease inhibitors. Some examples of the cellular targets which are inhibited by α-ketoamides are (i) thrombin, a serine protease that converts fibrinogen to fibrin;[10–12] (ii) calpain, a calcium-activated protease that has been implicated in strokes, Alzheimer's disease, and muscular dystrophy;[13–16] and (iii) caspase, a cystein protease that plays a role in programmed cell death.[17–20] Finding specific inhibitors for these proteases has become an important goal for the pharmaceutical industry. The traditional peptide-based inhibitors are inefficient due to the hydrolysis of the drug by a target protease or other nonspecific cellular peptidases. Novel inhibitors based on the α-ketoamide linkage are more stable towards the proteolytic cleavage, and pharmaceuticals based on this functionality are currently in the development and early testing phase.

It has been suggested that the high affinity of α-ketoamides towards proteases (for example, 1 pM in case of

*Corresponding author. Tel.: +1-805-893-2044; fax: +1-805-893-2229; e-mail: tcbruice@bioorganic.ucsb.edu

0968-0896/00/$ - see front matter
PII: S0968-0896(00)00122-X

thrombin inhibitor)[21] is related to the nonplanarity of the dicarbonyl group. The OC−CO dihedral angles are typically between 150° and 90° in the crystals of fully substituted α-ketoamides.[2,12,22] This twisted conformation is likely mimicking the tetrahedral transition state for the enzymatic peptide hydrolysis.[23,24] Nonplanar dicarbonyl group is present also in polyketides FK506 and rapamycin, both in solution and while bound.[3,25,26] Ab initio calculations have been performed on *N*,*N*-dimethyl-α-ketopropanamide, which is one of the smallest α-ketoamides with the nonplanar OC−CO unit.[27,28] This compound has a twist angle of 134.3° at the HF/6-31(d) level, and it was postulated that the deviation from planarity arises because of the steric interactions between the methyl substituents.[27] The early ab initio and semiempirical work lead to the development of OPLS/Amber force field parameters for the α-ketoamide unit in the naturally occurring polyketides FK506 and rapamycin.[28]

However, it is known that many α-ketoamides and α-ketocarbonyls are planar. Microwave spectroscopy and ab initio calculations have conclusively shown that the simplest dicarbonyl, ethanedial (glyoxal), occurs as an equilibrium mixture of two planar conformations. The s-*trans* conformer of glyoxal is 4.45 kcal/mol more stable than the s-*cis* conformer and the rotation around the OC−CO bond faces significant energy barrier with a transition state at about 75°.[29–31] Ab initio calculations at the HF/6-31(d) level predict that the simplest α-ketoamide, 2-oxoethanamide, is also planar.[27] During our work with the OPLS force field, we found that although good results were obtained for some nonplanar ketoamides, the current OPLS parameters failed to reproduce the geometries of simple planar α-ketoamides and α-ketocarbonyls. Also, experiments have shown that bound polyketides differ conformationally from free molecules,[32] and knowledge of the torsional energy as a function of the OC−CO dihedral angle is critical for the accurate prediction of binding energies of FK506 analogues to proteins FKBP12 and FKBP52. These considerations prompted the current study with a goal to develop a set of empirical parameters that describe accurately the torsional profiles of both the small planar α-ketoamides and substituted ketoamides with twisted diketone units. We now report the MP2/aug-cc-pVDZ geometries, torsional barriers, and conformer energies for several diketones and α-ketoamides. The present study also provides further understanding of the factors which determine the structure of the ketocarbonyl moiety.

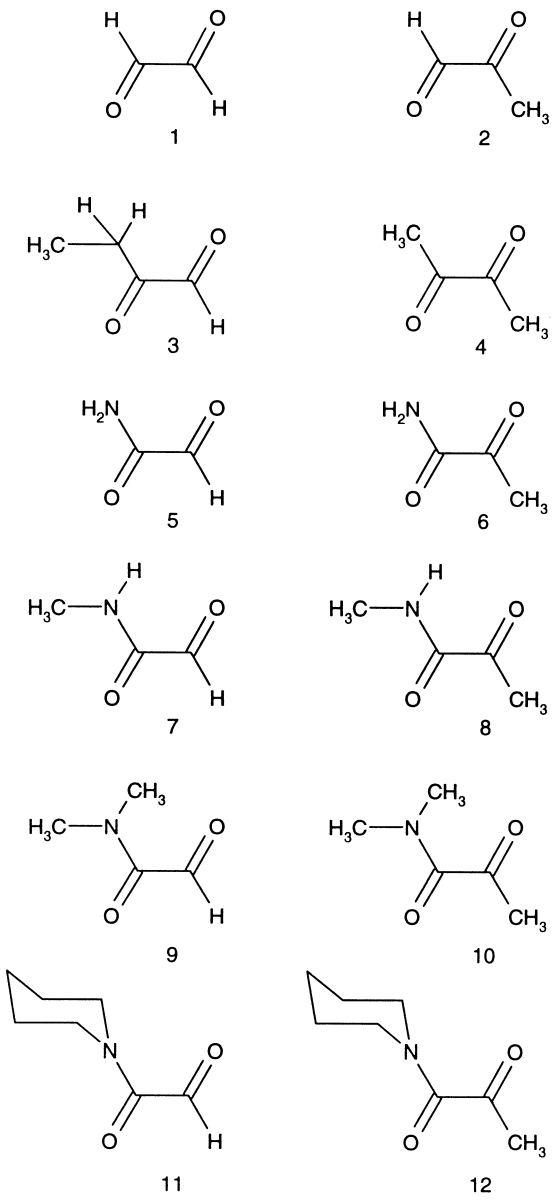

Scheme 2.

Results

MP2 and MP3 calculations. The conformational analysis of eight ketoamides and four diketones (Scheme 2) was performed as described in Computational Methods. The structures for the MP2(Full)/aug-cc-pVDZ minima of ethanedial (**1**), 2-oxopropanal (**2**), 2-oxobutanal (**3**), 2,3-butanedione (**4**), 2-oxoethanamide (**5**), 2-oxopropanamide (**6**), *N*-methyl-2-oxoethanamide (**7**), *N*-methyl-2-oxopropanamide (**8**), *N*,*N*-dimethyl-2-oxoethanamide (**9**), and *N*,*N*-dimethyl-2-oxopropanamide (**10**) are summarized in Table 1. Comparison of calculated and experimental vibrational frequencies for glyoxal is shown in Table 2. For compounds **1** and **4**, where experimental data are available, good agreement with calculated bond lengths, bond angles, rotational constants and vibrational frequencies is observed.[29,31,33–35] The largest discrepancy was found in the C=O bond length where the calculated distance in the s-*trans* ethanedial was 0.02 Å longer than the experimental. It has been reported that calculations at the CISD/DZ+P or CCSD/TZ2P level reproduce the experimental C=O bond length, and thus the MP2 result is in slight error.[31,36] We found that the MP3/aug-cc-pVDZ optimization reproduces the experimental and CCSD/TZ2P structures of **1** very well, and the MP3 optimization was also used to obtain more accurate structures for **3**, **5**, and **7** (Fig. 1). It should be noted that a good performance of the MP3 calculations is a feature of double-ζ basis set.[37] The experimental, HF and MP2 energy profiles describing the rotation

Table 1. Bond distances and bond angles for the *trans* (t) and *cis* (c) minima of the dicarbonyl unit from the MP2(Full)/aug-cc-pVDZ optimization. The structures of **1**, **2**, **5** and **7** at the MP3(Full)/aug-cc-pVDZ level are shown in Figure 1 for comparison

	C–C	C_H–O	C_{CT}–O	C–H	C–CT	C–C–H	C–C–CT	O–C–H	O–C–CT
1t	1.522	1.225	—	1.112	—	115.4	—	123.2	—
2t	1.531	1.225	1.231	1.113	1.504	114.1	117.5	123.0	124.9
3t	1.532	1.225	1.231	1.113	1.507	114.0	117.7	122.9	124.8
4t	1.543	—	1.231	—	1.506	—	116.8	—	124.1
1c	1.539	1.220	—	1.115	—	115.3	—	122.1	—
2c	1.548	1.220	1.225	1.116	1.510	116.0	115.7	121.4	124.4
3c	1.546	1.221	1.225	1.116	1.512	115.9	115.5	121.4	124.4
4c[a]	1.563	—	1.225	—	1.514	—	118.4	—	122.7
	C–C	C_N–O	C_R–O	C–N	C–R	C–C–N	C–C–R	O–C–N	O–C–R
5t	1.529	1.234	1.225	1.357	1.109	113.6	113.9	126.3	123.2
6t	1.542	1.235	1.231	1.357	1.502	112.9	115.9	125.7	124.4
7t	1.526	1.239	1.226	1.352	1.110	114.1	114.0	125.5	123.0
8t	1.539	1.240	1.232	1.352	1.502	113.4	115.9	124.9	124.2
9t	1.528	1.244	1.226	1.358	1.111	119.9	111.8	125.0	122.3
10t	1.535	1.244	1.231	1.361	1.506	118.3	115.1	124.6	123.9
5c	1.539	1.226	1.218	1.370	1.117	112.6	116.3	124.8	121.4
6c	1.554	1.226	1.223	1.373	1.517	115.3	119.2	123.3	122.4
7c	1.534	1.231	1.219	1.365	1.118	112.9	116.0	123.9	121.2
8c	1.550	1.232	1.224	1.367	1.518	115.7	119.3	122.6	122.1

[a]4c is not a minimum but a transition state.

Table 2. MP2/aug-cc-pVDZ normal mode frequencies in cm^{-1} for the s-*trans* and s-*cis* minima, and for the transition state in ethanedial (**1**) and 2-oxoethanamide (**5**)

	Ethanedial[a]			2-Oxoethanamide		
Mode	*trans*	*cis*	TS	*trans*	*cis*	TS
C–C torsion	129 (127)	85 (91)	166i	137	101	118i
C–N torsion				659	644	569
NH wag (pyram.)				328	212	283
CN wag (impr.)				539	499	482
CH wag (impr.)	816 (801)	735	823			
CH wag (impr.)	1061 (1048)	1056 (1049)	992	1007	979	964
CCO bend	335 (339)	281 (285)	296	277	275	279
CCO bend	558 (551)	817	462	485	418	330
NCC bend				594	673	732
HNC bend				1081	1070	1086
HCC bend	1325 (1312)	1378	1373			
HCC bend	1367 (1353)	1386	1394	1347	1420	1411
HNH bend				1600	1621	1623
C–C stretch	1106 (1066)	866 (826)	1072	907	847	895
C–N stretch				1395	1310	1322
C–O stretch	1702 (1732)	1739	1709	1712	1739	1725
C–O stretch	1718 (1744)	1705 (1746)	1729	1762	1773	1753
C–H stretch	3029 (2809)	2967	2971	3054	2948	2976
C–H stretch	3033 (2835)	2995	2987			
N–H stretch				3597	3604	3587
N–H stretch				3753	3755	3737

[a]For ethanedial: experimental values are given in parenthesis.

around the carbon–carbon single bond in ethanedial are shown on Figure 2a. The agreement between the ab initio MP2 data and experimental torsional potential is excellent, but the HF/aug-cc-pVDZ profile overestimates the energy of the s-*cis* isomer. Overestimation relative to the MP2 profile is seen also in the HF/aug-cc-pVDZ rotational profiles of **2** (data not shown) and **5** (Fig. 3a), indicating that the electron correlation effects contribute significantly to the stabilization of the s-*cis* arrangement of two carbonyl groups. Thus, α-ketocarbonyls, and α-ketoamides represent systems where an accurate treatment of electron correlation is required for the correct description of the rotational profile. Neglecting electron correlation effects would lead to qualitatively incorrect results, e.g. failure to predict a stable minimum for *cis* 2-oxopropanamide.

Dicarbonyls **1** and **2** (Fig. 1), and ketoamides **5** and **6** (Fig. 4-(**5**) and 4-(**6**)) possess two conformational minima, corresponding to the 180° rotation around the OC–CO bond. Four stable conformations were found for dicarbonyl **3** that possesses an additional degree of freedom around the CC–CC bond. In dicarbonyl **4**, the steric repulsion of the two methyl groups caused the s-*cis* conformation to be a saddle point rather than a minimum and for this molecule only one stable conformation exists. Secondary α-ketoamides **7** and **8** (Fig. 4-(**7**) and 4-(**8**)) have additional minima (structures not shown) corresponding to the *cis* conformation of the amide bond. For dicarbonyls **1**–**4**, and for ketoamides **5**–**8**, the conformation with two carbonyl groups in s-*trans* was always lower in energy than the corresponding s-*cis* conformation. The tertiary ketoamides **9** and **10** (Fig. 4-(**9**) and 4-(**10**)) are examples of nonplanar ketoamides where the s-*trans* arrangement of carbonyl groups is a transition state connecting two equivalent minima. The large nonsymmetric ketoamides **11** and **12** have two nonequivalent minima as illustrated in Figure 5 for molecule **11**. The pipecoyl ring in **11** and **12** prefers the chair conformation; the boat form was not an energy minimum.

The internal rotation around the carbon–carbon single bond in dicarbonyls is coupled to the remaining degrees of freedom. Significant skeletal relaxation takes place during the rotation, and the systematic variations in bond lengths during the rotation around the OC–CO bond are shown in panels b and c of Figures 2 and 3. It has been shown recently that such skeletal relaxation plays an important role in determining the energy profile for the

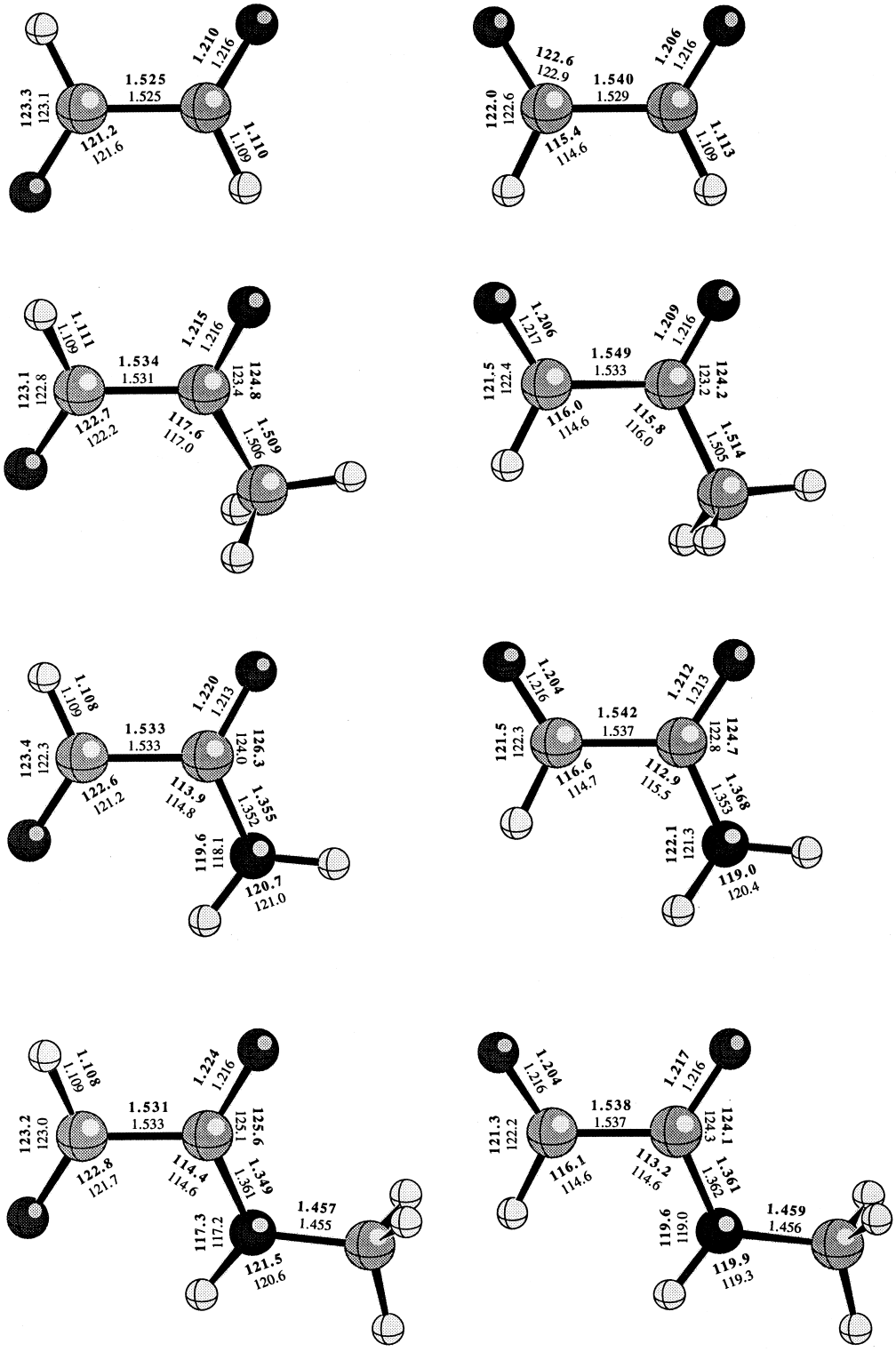

Figure 1. Comparison of MP3/(Full)/aug-cc-pVDZ (**Bold**) and OPLS-AA (normal) structures for s-*cis* and s-*trans* conformers of ethanamide, 2-oxopropanal, 2-oxopropanal, 2-oxoethanamide, and *N*-methyl-2-oxoethanamide.

rotation around the single bonds.[38] Fitting the electrostatic potential with atom-centered point charges showed that the charge distribution is sensitive to the torsional degree of freedom. In the s-*cis* ketoamide, the amide carbon and amide nitrogen have largest positive and negative partial charges, respectively. In the s-*trans* form, both the carbon and nitrogen atoms carry less charge. The amide nitrogen was planar in s-*cis* and s-*trans* forms of ketoamides **5**, **6**, **7** and **8**, but the nitrogen center becomes pyramidal when the OC−CO torsional angle deviates from 0° or 180°. To further investigate how the OC−CO internal rotation affects the bonding in ketoamides, MP2/aug-cc-pVDZ normal mode frequencies were calculated for the two minima and for the rotational

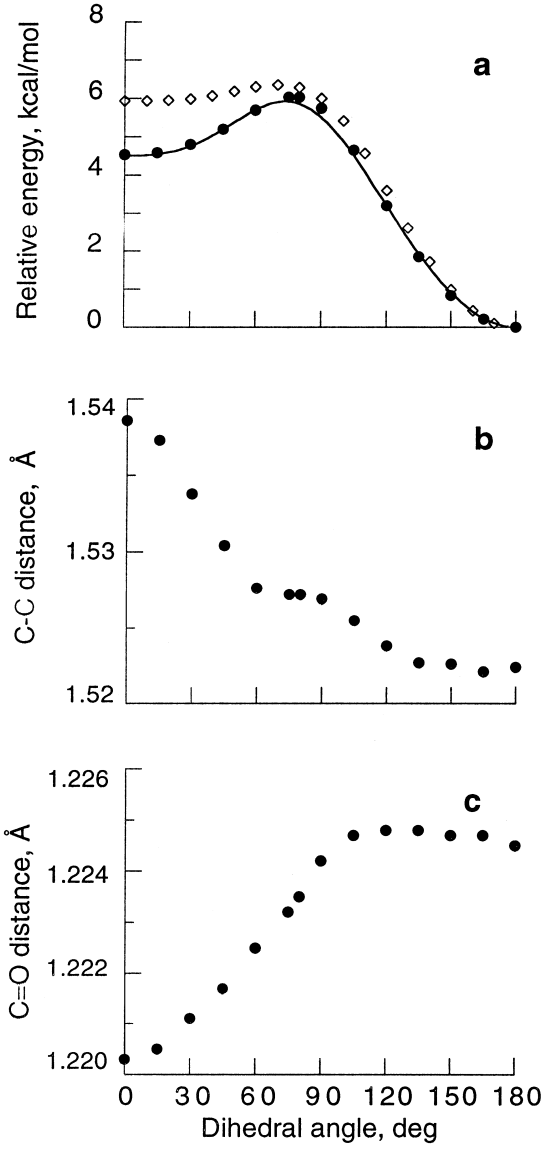

Figure 2. Internal rotation in ethanedial (**1**). MP2/aug-cc-pVDZ (closed circles), HF/aug-cc-pVDZ (open diamonds), and experimental (solid line) energies for the internal rotation around the OC–CO bond (panel a). Changes in the carbon–carbon (panel b) and carbon–oxygen (panel c) bond lengths during the internal rotation. Experimental profile was obtained from ref 29.

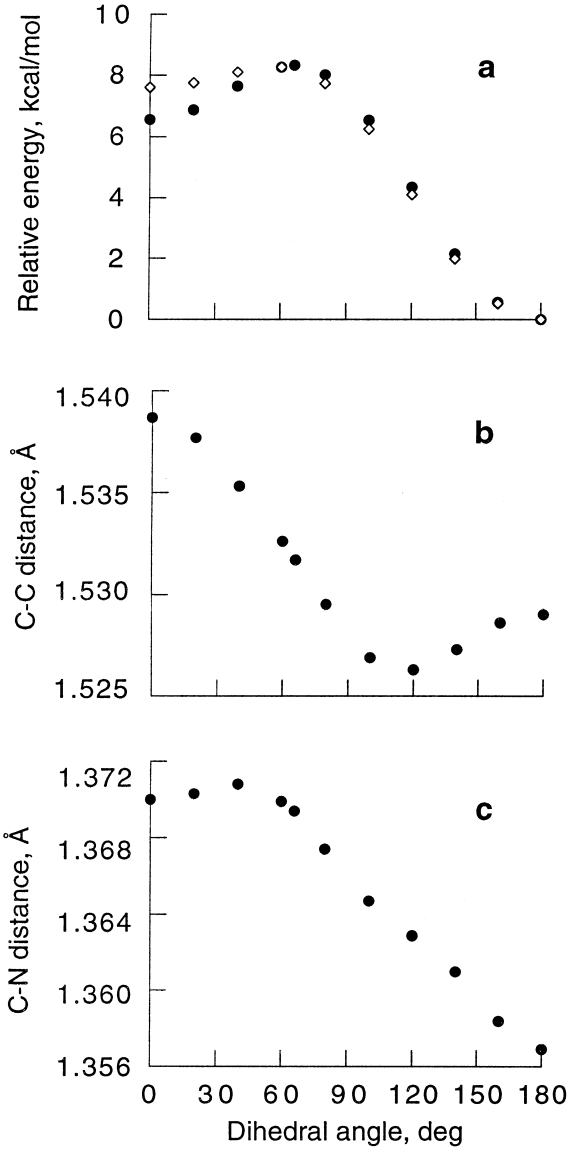

Figure 3. Internal rotation in 2-oxoethanamide (**5**). MP2/aug-cc-pVDZ (closed circles) and HF/aug-cc-pVDZ (open diamonds) energies from the internal rotation around the OC–CO bond (panel a). Changes in the carbon–carbon (panel b) and carbon–nitrogen (panel c) bond lengths during the internal rotation.

transition state in **5.** Table 2 shows that the carbon–nitrogen bond stretching frequency, carbon–nitrogen out-of-plane torsional frequency (CN wag), and the frequency for pyramidalization of amide nitrogen (NH wag) are largest in the s-*trans* conformer of 2-oxoethanamide. Similar results (data not shown) were observed for ketoamides **6** and **7**.

The methyl group in dicarbonyl **2** prefers eclipsing conformation and the barrier for the rotation of the methyl group was 0.85 kcal/mol at the MP2/aug-cc-pVDZ level. It should be noted that the calculated $C(sp^2)$-$C(sp^3)$ rotational barriers have been shown to be strongly method dependent in case of acetamide,[39,40] and we calculated the methyl rotation barrier in **2** also at the MP2(Full)/aug-cc-pVTZ, MP3(Full)/aug-cc-pVDZ and MP3(Full)/aug-cc-pVTZ levels. The MP3 calculation with the double-ζ basis set was in good agreement (0.89 kcal/mol) with the MP2 result but the calculations using the triple-ζ basis set yielded lower barriers, 0.57 and 0.60 kcal/mol, for the MP2 and MP3, respectively. The rotation of the ethyl group in **3** faces a barrier of 4.64 kcal/mol when the CC–CC angle is 0 degrees; the methyl barrier in **3** was 2.83 kcal/mol at the MP2/aug-cc-pVDZ level. The rotation barrier for the *N*-methyl group in ketoamide **7** is underestimated (0.03 kcal/mol) at the MP2/aug-cc-pVDZ level[41] and a more accurate value of 0.14 kcal/mol from MP2/6-311 + G(d,p) single point calculations was used to assign the CG–N–CT–HC torsional potential. For comparison, the torsional potential for the methyl group in N-methylformamide is 0.17 kcal/mol.[42]

OPLS Parameters. The development of parameters for diketones and ketoamides was performed in an iterative

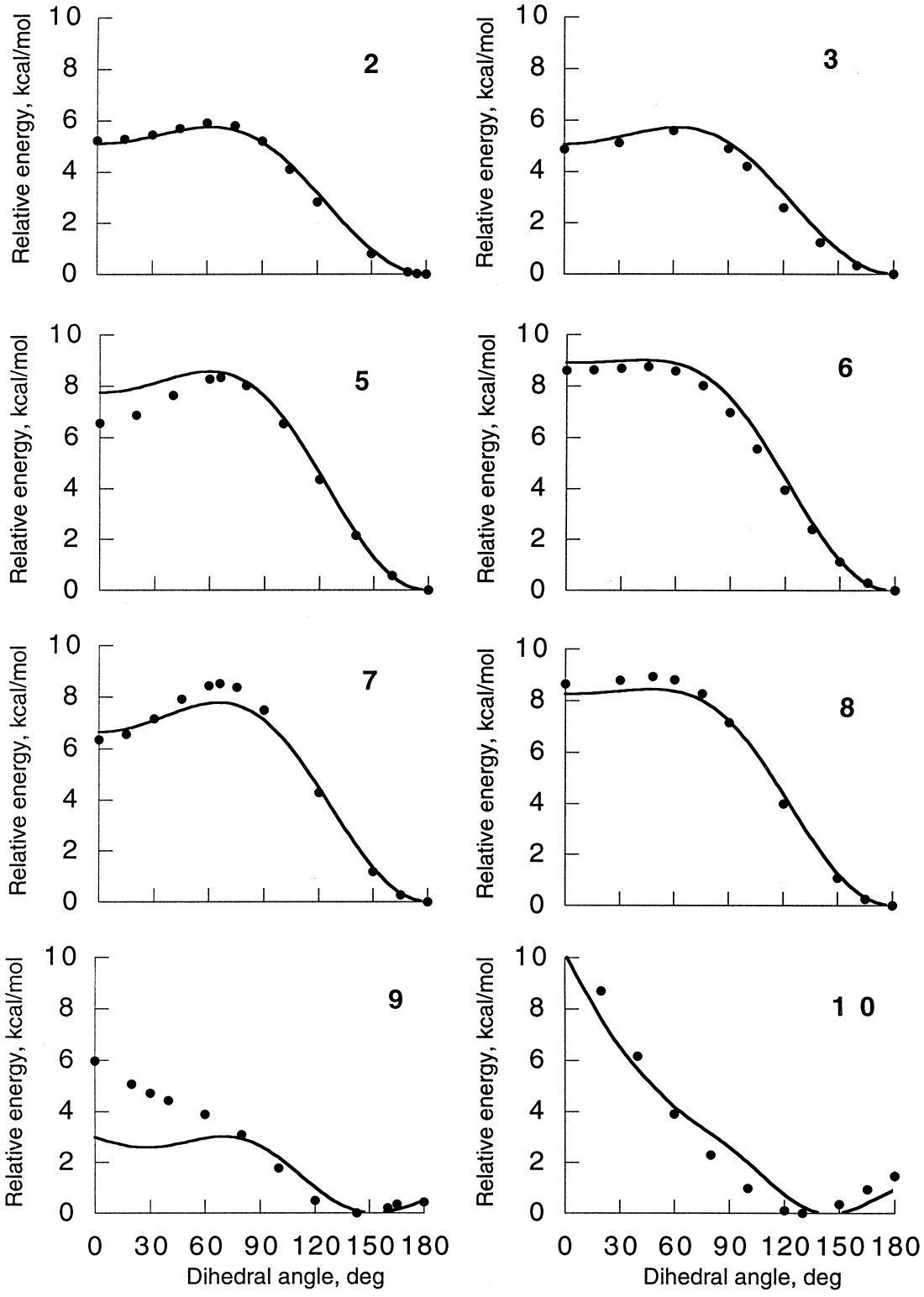

Figure 4. Comparison of MP2 (closed circles) and OPLS-AA (solid line) torsional energy profiles for 2-oxopropanal (**2**), 2-oxobutanal (**3**), 2-oxoethanamide (**5**), 2-oxopropanamide (**6**), *N*-methyl-2-oxoethanamide (**7**), *N*-methyl-2-oxopropanamide (**8**), *N*,*N*-dimethyl-2-oxoethanamide (**9**), and *N*,*N*-dimethyl-2-oxopropanamide (**10**).

manner starting with the assignment of atomic charges to carbonyl carbons, carbonyl oxygens, amide nitrogen, and to carbons connected to amide nitrogen. It was found that the default OPLS charges and Lennard–Jones parameters for carbonyl group describe well diketones and ketoamides and only minor modifications were necessary. This is not surprising given that a considerable effort has been put into developing the OPLS-AA force field.[28,43,44] However, the charge at the tertiary nitrogen was modified from its default value (−0.14) to −0.28.

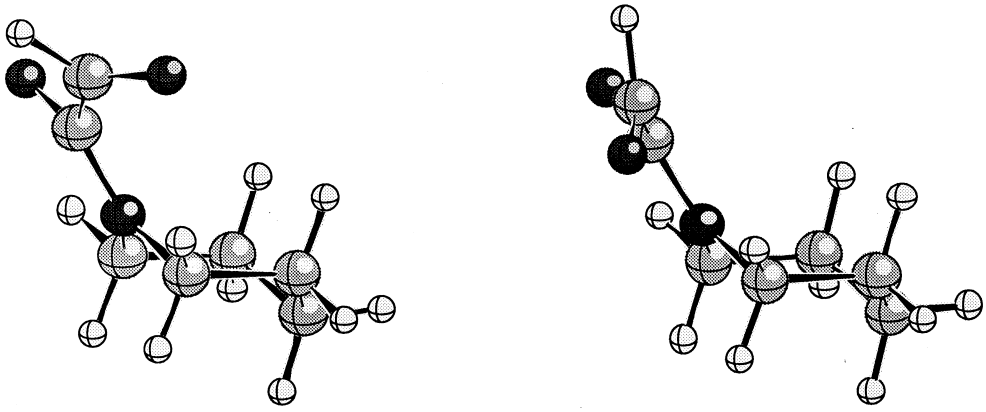

Figure 5. Two nonequivalent conformations of tertiary ketoamide **11** at the MP2(Full)/6-31 + G(d,p) level. Similar conformations were also found for the ketoamide **12**.

This provided good match to the CHelpG and RESP charges and reproduced well the MP2 interaction potential between the water molecule and ketoamide **9**. It should be noted, that the tertiary nitrogen charge was previously reduced from −0.56 to −0.14 in order to reproduce the heat of vaporization of *N*,*N*-dimethylacetamide (DMA).[43] We found that the bulk properties of DMA can be reproduced very well with a charge of −0.28 when the Lennard–Jones ϵ for the *N*-methyl hydrogens is reduced.[44] The combination of Q(N) = −0.28 and ϵ (H at N−CH_3) = 0.02 gives d^{25} of 0.914±0.001 g/cm^3 and ΔH_{vap} of 11.80±0.04 kcal/mol. The experimental density of DMA is 0.936 g/cm^3 while the values of 11.75, 10.9 and 12.0 kcal/mol have been reported for the experimental ΔH_{vap}.[43,45] The final OPLS−AA charges and Lennard–Jones parameters for the ketoamide moiety are listed in Table 3. These nonbonded parameters, along with the bond stretching and bond bending parameters shown in Table 4 yielded OPLS-minimized structures and vibrational frequencies that reproduced closely the corresponding MP2 and MP3 results (typical results for structures are shown in Fig. 1). The torsional potential in the OPLS−AA force field, as currently implemented in the program BOSS, has the following form:[43]

$$E_{\text{torsion}} = \sum_i \frac{V_1^i}{2}[1 + \cos(\phi_i)] + \frac{V_2^i}{2}[1 - \cos(2\phi_i)] + \frac{V_3^i}{2}[1 + \cos(3\phi_i)] \quad (1)$$

Two sets of torsional parameters for ketoamide have been reported previously. The original parametrization[28] used only V_1 and V_2 terms and was derived based on the HF/6-31G(d)//3-21G profile for the ketoamide **9**. At this level of theory, the barrier for rotation through the s-*cis* conformation was predicted to be about 12.5 kcal/mol which is 1 kcal/mol higher than the current MP2/aug-cc-pVDZ barrier. The two methods also give minima at similar values of the OC−CO dihedral angle

Table 3. OPLS-AA nonbonded parameters for α-ketocarbonyls and α-ketoamides. Most ϵ and σ values are taken from the standard OPLS-AA force field.[43]

Type	Q	ϵ	σ	Description
CG	+0.40	3.75	0.105	C: C=O keto in α-ketoamide
CG	+0.49	3.75	0.105	C: C=O amide in α-ketoamide
O	−0.40	2.96	0.210	O: C=O keto in α-ketoamide
O	−0.49	2.96	0.210	O: C=O amide in α-ketoamide
N	−0.74	3.25	0.170	N: primary amide in α-ketoamide
N	−0.50	3.25	0.170	N: secondary amide in α-ketoamide
N	−0.28	3.25	0.170	N: tertiary amide in α-ketoamide
CT	−0.18	3.50	0.066	C: CH_3 bonded to a carbonyl carbon
CT	+0.02	3.50	0.066	C: CH_3 on N in secondary α-ketoamide
CT	−0.04	3.50	0.066	C: CH_3 on N in tertiary α-ketoamide
HC	+0.06	2.42	0.015	H on C: CH_3 bonded to a carbonyl carbon
HC	+0.06	2.50	0.020	H on C: CH_3 directly bonded to N
HC	+0.06	2.50	0.030	H on C: alkanes
H	+0.37	0.00	0.000	H on N: primary ketoamide
H	+0.30	0.00	0.000	H on N: secondary ketoamide

Table 4. OPLA-AA bond stretching and bond bending parameters for the ketoamide moiety. The bond stretching force constant K_r is in kcal/(mol·Å^2) and the bond bending force constant K_θ is in kcal/(mol·radian^2)

Bond	K_r	R(Å)
CG−CG	300.0	1.521
CG−O	700.0	1.215
CG−HC	314.0	1.109
CG−CT	317.0	1.503
CG−N	460.0	1.357
H−N	434.0	1.010
CT−N	380.0	1.449
Angle	K_θ	θ (deg)
CG−CG−HC	42.0	114.0
CG−CG−O	70.0	120.5
CG−CG−CT	70.0	117.0
CG−CG−N	70.0	115.0
O−CG−HC	50.0	122.2
O−CG−CT	80.0	125.0
O−CG−N	80.0	126.0
CG−CT−HC	37.0	109.0
CG−CT−CT	63.0	111.1
CG−N−H	37.0	119.4
CG−N−CT	50.0	119.5
CT−N−CT	50.0	120.0
CT−N−H	35.0	118.4
H−N−H	31.0	117.0
CT−CT−N	80.0	115.2
HC−CT−N	35.0	109.5

(135° for HF and 130.1° for MP2) suggesting that the original parameters were appropriate for tertiary ketoamides such as FK506. In the more recent parameter set[46] the nonplanarity of ketoamides was influenced by the presence of V_3 term which leads to the artificial twisting of small dicarbonyl compounds. The V_3 torsional term in the current force field (Table 5) is zero, resembling thus the original parameter set. This means that the nonplanarity of ketoamides arises entirely from nonbonded interactions. The comparison of the OPLS and MP2 torsional profiles for ketoamides **5**–**10** is shown in Fig. 4. The OPLS-AA calculations reproduce well the rotational energy profile for all molecules but **9**, where OPLS predicts the presence of a high-energy conformer. The OPLS calculations also nicely reproduce the two nonequivalent minima for pipecoyl-substituted dicarbonyls **11** and **12**. For compound **11**, the OPLS-AA predicted minima for rotation around the OC−CO bond occur at −141.7° and +142.8°, compared to −139.9° and +144.0° at the MP2(Full)/6-31+G(d,p) level. The OPLS values for the tertiary ketoamide **12** are −136.3° and +137.5° while MP2(FC)/6-31+G(d,p) calculated minima lie at −126.8° and +127.5°.

Discussion

Electronic structure of dicarbonyls and ketoamides. The origin of the barrier for the rotation around the carbon−carbon single bond in ketocarbonyl compounds has been of considerable interest in the past.[36,47–49] In particular, "the presence of significant barrier between the s-*cis* and s-*trans* rotamers of glyoxal remains somewhat a mystery. The calculated charges, bond orders, delocalization indices, and intuition all suggest that any π-delocalization interaction should be very weak".[49] It is well accepted that the main factor contributing to the energy difference between the s-*cis* and s-*trans* conformers is the repulsion of oxygen lone pairs.[36] Not so well understood are the reasons for changes in bond lengths as the rotation around the carbon−carbon single bond occurs.[33] Data in Table 1 indicate that the C−C bond is longer and the C=O bond is slightly shorter when the two carbonyl oxygens are *cis*. These trends are consistent with the previous high level CISD/DZ+P, CCSD/TZ2P, and MP4(SDQ)/6-311+G** ab initio calculations of glyoxal.[31,36,50] The bond length changes can be rationalized when one considers that the interaction of two carbonyl dipoles is one of the major factors determining the conformation of ethanedial. The CHelpG charges indicate a reduction of the negative charge at the oxygen atom in the transition state and in the s-*cis* form compared to the s-*trans* form. The decrease of the local C−O dipole moment in s-*cis* ethanedial leads to a decreased dipole-dipole repulsion between the two carbonyl groups and lowers the energy of *cis*-ethanedial. Analysis of bond distances and stretching force constants further suggests that the double-bond character of the carbon–oxygen bond increases slightly as *trans* glyoxal converts to the *cis* form. Figures 2 and 3 (panel b) illustrate that the carbon−carbon bond becomes longer in *cis* dicarbonyls so that the oxygen lone pair repulsion would be smaller. The importance of electron correlation in describing correctly the energy of *cis*-ethanedial has been noted previously.[36,50] Figure 2a shows that at the HF level, *cis*-ethanedial is unstable, but inclusion of the dynamic electron correlation via the MP2 treatment leads to the stabilization of the s-*cis* conformer. The UNO-CAS calculations have shown that the nondynamic electron correlation plays only minor role in glyoxal, thus the exited configurations are not important in the stability of *cis* glyoxal.[51] It is likely that the stabilizing effect observed in the MP2 calculations arises from the dispersion attractions between two adjacent hydrogen and two adjacent oxygen atoms in *cis* glyoxal.

Analysis of interatomic distances in Table 1 and Figures 1–3 reveals that similar structural trends are also found in α-ketoamides. The C−C bond is typically 1.52–1.54 Å in s-*trans* conformers and 1.54–1.55 Å in s-*cis* forms. The bond length in twisted intermediate geometries is never longer than in the s-*cis* and s-*trans* conformers, suggesting that there is no resonance contribution to interaction between the two carbonyl groups. Instead, the lengthening of the bond in s-*cis* compounds can be attributed to the increased electrostatic repulsion between the two carbonyl oxygens. The electrostatic nature of the C−C bond elongation is further supported by the finding that this trend was present in the OPLS calculated geometries of s-*cis* and s-*trans* ketoamides. Although the two carbonyl groups in the planar α-ketocarbonyl compounds are geometrically aligned so that conjugation of double bonds can occur, the role of resonance stabilization in the formation of planar structures appears to be small.

Table 5. Fourier coefficients (in kcal/mol) for the improper dihedrals and torsional dihedrals in ketocarbonys and ketoamides

Improper	V_1	V_2	V_3
O−CG−HC−CG	0.0	20.2	0.0
O−CG−CT−CG	0.0	18.0	0.0
O−CG−N−CG	0.0	16.5	0.0
H−CG−N−H (prim.)	0.0	−3.4	0.0
H−CG−N−CT (sec.)	0.0	−1.7	0.0
CT−CG−N−CT (tert.)	0.0	0.0	0.0
Torsion	V_1	V_2	V_3
O−CG−CG−O	1.6	3.2	0.0
O−CG−CG−HC	0.0	0.2	0.0
O−CG−CG−CT	0.0	0.5	0.0
HC−CG−CG−HC	0.8	0.0	0.0
CT−CG−CG−HC	0.8	−0.6	0.0
CT−CG−CG−CT	0.7	−1.5	0.0
HC−CT−CG−CG	0.0	0.0	0.085
HC−CT−CG−O	0.0	0.0	−0.085
N−CG−CG−O	0.0	0.0	0.0
N−CG−CG−HC	−0.9	0.3	0.0
N−CG−CG−CT	−0.5	0.2	0.0
H−N−CG−CG	0.0	4.9	0.0
H−N−CG−O	0.0	4.9	0.0
CT−N−CG−O	−0.4	4.9	0.0
CT−N−CG−CG	0.4	4.9	0.0
CT−N−CT−HC	0.0	0.0	0.65
CG−N−CT−HC	0.0	0.0	−0.09
O−CG−CT−CT	0.0	0.0	0.0
CG−CG−CT−CT	−2.0	0.75	0.4

The amide carbon–nitrogen bond was 1.352–1.361 Å in s-*trans* ketoamides, which is slightly shorter than the experimentally determined amide bond in typical gaseous amides.[52–54] The short C–N amide distance, significant barrier for the rotation around the amide bond, and lack of conjugation between the two carbonyl groups indicate that α-ketoamides can be viewed as amides which have been substituted by an electron-withdrawing carbonyl group. However, the interaction of amide group with the adjacent keto group has the following important consequences: (i) an elongation of the amide bond by 0.014 Å occurs when the two carbonyl groups are in s-*cis* conformation (Figs 1 and 3c), (ii) the pyramidalization at amide nitrogen occurs when the OC–CO bond became significantly twisted, and (iii) the force constants indicate substantial weakening of the C–N bond when the OC–CO dihedral differs from 180°. Finally, the CHelpG charges show that nitrogen is more negatively charged in the s-*cis* conformation and in the TS compared to the lowest energy s-*trans* conformation. The change in bonding as the rotation around the OC–CO bond occurs can be rationalized as the decreased contribution of the resonance form where the nitrogen atom is formally double bonded to carbon.[55] The classical amide resonance form (B in Scheme 3) is significant in s-*trans* ketoamides because it minimizes the electrostatic repulsion between negatively charges nitrogen and the distal oxygen. The carbonyl dipolar structure (C in Scheme 3) becomes more important as the OC–CO bond is rotated out of the 180° minimum. The carbonyl dipolar resonance form could be significant in normal amides unless neighboring electrostatic effects stabilize the classical amide resonance structure.

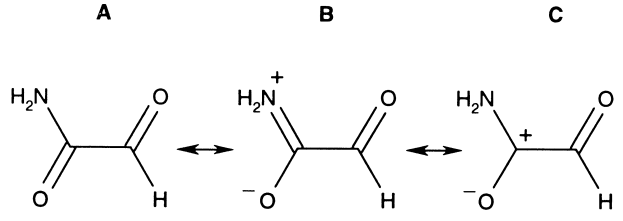

Scheme 3.

The nonplanarity of a dicarbonyl unit arises when at least one of the substituents is a bulky group. For example, **9** and **11** are nonplanar despite the presence of hydrogen at one of the carbonyl groups. In this case, the nonplanarity is caused by an unfavorable steric interaction between the bulky substituent and the distal oxygen. It has been suggested previously that the nonplanarity of substituted ketoamides results from steric interaction between two substituents.[27] Current data favor a model where the repulsion between two substituents destabilizes the s-*cis* conformation of ketoamides, but interaction between the keto oxygen and a bulky substituent causes the destabilization of the s-*trans* form.

Implications for the rational design of ketoamide-based inhibitors. The α-ketoamide moiety is an important building block in protease inhibitors,[14] neuroregenerative or immunosuppressive polyketides,[1] and in the macrolide antitumor antibiotic lankacidin.[56] The knowledge of its structural properties will be helpful for rational drug design. Although the structure, and conformer energies of most ketoamides can be determined with the current OPLS parameters, some general structural features will be summarized below. The α-ketoamide unit prefers geometry where the nitrogen atom and two carbonyl groups are all in the same plane and the two oxygen atoms are in *trans*. If the nitrogen in α-ketoamide is monosubstituted by an aliphatic chain, the amide bond prefers *trans* orientation. The barrier for rotation around the amide bond in ketoamides is similar to normal amides; the rotational barrier around the OC–CO bond is typically 5–10 kcal/mol. Tertiary ketoamides possess nearly planar nitrogen center but the ketoamide unit becomes nonplanar. The compounds with general structure R(bulky)–CO–CHO adopt the OC–CO dihedral angle close to 140–150°. The compounds with central dicarbonyl group (e.g. R(bulky)–CO–CO–R) are more twisted, with the OC–CO dihedral near 100–140°.

Conclusions

The present study provides high level ab initio structural data about the ketocarbonyl and ketoamide moieties which are present in many potent protease inhibitors. The energy profiles for the internal rotation around the OC–CO bond have been determined at the MP2/aug-cc-pVDZ and MP2/6-31 + G(d,p) levels. The main factor which determines the rotational profile in simple α-ketoamides and α-ketocarbonyls is the electrostatic dipolar interaction between the two carbonyl groups. There is no evidence for resonance conjugation of the two adjacent carbonyl groups, but the electrostatic effects cause a significant change in hybridization at the amide nitrogen as the rotation around the OC–CO single bond occurs. The ab initio results have been used to obtain a new set of OPLS charges, stretching and bending parameters and torsional potentials which can be used for a wide range of compounds containing the OC–CO moiety. The main changes from the previous description of ketoamides are new torsional parameters and a new value for the charge at nitrogen in tertiary ketoamide.

Computational Methods

Ab initio quantum mechanical calculations were performed on α-ketoamides and α-ketocarbonyls (**1**–**12**) utilizing the program package GAUSSIAN98.[57] Dicarbonyls **1**–**4** and ketoamides **5**–**10** were optimized at the MP2(full)/aug-cc-pVDZ level, while the 6-31 + G(d,p) basis was used for the larger ketoamides **11** and **12**. Transition states for the OC–CO bond rotation in **1**, **5** and **7** were located using analytically calculated force constants. The s-*cis* and s-*trans* minima of **1**–**7** as well as transition states for **1** and **5** were verified by a subsequent frequency calculation at the MP2(full)/aug-cc-pVDZ level. The s-*cis* and s-*trans* conformers of **1**, **2**, **5** and **7** were also optimized at the MP3(full)/aug-cc-pVDZ level. The potential energy surface for dicarbonyls **1**–**4**, and ketoamides **5**–**10** was scanned by optimizing the rest of the molecule while the OC–CO dihedral was fixed to a given value.

For molecules **1**–**9**, the MP2(full)/aug-cc-pVDZ method was used while the torsional potential for **10** was determined a the MP2(full)/6-31 + G(d,p) level of theory. Typically, 8–10 steps between 0° and 180° were taken to obtain the torsional barrier for the rotation around the OC−CO bond. The amide bond in **6** and **7** was *trans* during these potential energy scans.

The electrostatic potential-derived charges were obtained at energy minima and at several points along the rotation profile using the CHelpG scheme. It was observed that in some instances, such as in the secondary ketoamide **7**, the CHelpG charges were conformation dependent. Because one of the goals of the present work was to derive OPLS force field parameters for ketoamides, conformation-independent charges were desirable. To obtain such charges, the electrostatic potential was calculated from the MP2 density using the Merz–Singh–Kollmann point selection scheme[58] with 8–12 layers using GAUSSIAN98. The program Resp[59] was then used to perform a restrained fit over multiple conformers. The charges on hydrogens, and of the methyl carbon connected to a carbonyl carbon, were fixed to values present in the OPLS-AA force field (CH_3 carbon has OPLS charge +0.18, CH_3 hydrogens each: −0.06, H in −CHO: 0.00).

All molecular mechanics calculations were performed with the program BOSS.[60] The parametrization of OPLS-AA force field for α-ketoamides was performed similarly to a suggested procedure.[43,61] Briefly, default Lennard–Jones parameters were used for all atoms, except for hydrogens attached to carbon directly bonded to nitrogen. The ϵ for these hydrogens was reduced to 0.020 in accord with a recent suggestion on improving the OPLS-AA force field for amines and amides.[44] The hydrogens on methyl carbons which are connected to the carbonyl group were treated as in ketones (e.g. the reduced Lennard–Jones ϵ of 0.015 kcal/mol was used). A new atom type, CG for two adjacent carbonyl carbons, was created to avoid affecting the peptide bond parameters during the assignment of ketoamide parameters. This atom type was assigned Lennard–Jones and SASA parameters of the AMBER type C as in ketones and amides.[62] A consistent set of atomic charges for carbons, oxygens, and nitrogen were obtained from the RESP fitting, as described above. The charge at the nitrogen atom of tertiary ketoamide was not well defined by the CHelpG calculations, and additional fitting to the water–**9** interaction energy profile was performed. The reference profile was calculated at the MP2/aug-cc-pVDZ level and corrected for the basis set superposition error by means of counterpoise correction.[63,64] The value derived from the fitting, −0.28 *e*, was further tested by performing bulk solvent simulation on *N*,*N*-dimethylacetamide as described previously.[43]

The default OPLS-AA parameter set does not provide parameters for the bending of the ketoamide unit as well as for the stretching of the OC−CO bond. These parameters were estimated by fitting the OPLS derived frequencies of **1**, **2**, **5**, **6**, **7** to the corresponding MP2/aug-cc-pVDZ frequencies and to the experimental IR spectrum of **1**. A set of new torsional parameters describing the rotation around the OC−CO was created by fitting the OPLS-AA rotational profiles to the corresponding MP2(full)/aug-cc-pVDZ profiles for compounds **1-10**. Additionally, the OC−CH_3, CH_2−CH_3, and OC− CH_2R barriers were determined for s-*trans* **2** and s-*trans* **3** at the MP2(full)/aug-cc-pVDZ level of theory. The torsional barrier around the CN-CH_3 bond in s-*trans* **6** was estimated at the MP2/aug-cc-pVDZ and MP2(full)/6-311 + G(d,p) levels. The quality of the new torsional parameters was tested by comparing the OPLS and MP2 minimum energy structures for compounds **11** and **12**.

Acknowledgements

This research was supported by a grant BA1-9904-2 from the Christopher Reeve Paralysis Foundation. The computational resources were provided partially by National Computational Science Alliance and UCSB's Supercomputer Facility. The latter is supported by grants from NSF (CDA96-01954) and Silicon Graphics Inc. We are also thankful for Kosan Biosciences, Inc. for a continual support of our computational facilities. The authors thank Dr. Bernie Kirtman for the critical reading of the manuscript and Dr. Helgi Adelsteinsson for helpful discussions.

References and Notes

1. Schreiber, S. L. *Science* **1991**, *251*, 283.
2. Tanaka, H.; Kuroda, A.; Marusawa, H.; Hatanaka, H.; Kino, T.; Goto, T.; Hashimoto, M.; Taga, T. *J. Am. Chem. Soc*. **1987**, *109*, 5031.
3. Swindells, N. D. C.; White, P. S.; Findlay, J. A. *Can. J. Chem*. **1978**, *56*, 2491.
4. Hamilton, G. S.; Steiner, J. P. *J. Med. Chem*. **1998**, *41*, 5119.
5. Siekierka, J. J.; Hung, S. H.; Poe, M.; Lin, C. S.; Sigal, N. H. *Nature* **1989**, *341*, 755.
6. Harding, M. W.; Galat, A.; Uehling, D. E.; Schreiber, S. L. *Nature* **1989**, *341*, 758.
7. Gold, B. G.; Densmore, V.; Shou, W.; Matzuk, M. M.; Gordon, H. S. *J. Pharm. Exp. Therapeut*. **1999**, *289*, 1202.
8. Adelsteinsson, H.; Bruice, T. C. *Bioorg. Med. Chem*. **2000**, *8*, 617.
9. Adelsteinsson, H.; Bruice, T. C. *Bioorg. Med. Chem*. **2000**, *8*, 625.
10. Di Cera, E.; Dang, Q. D.; Ayala, Y. M. *Cell. Mol. Life Sci*. **1997**, *53*, 701.
11. Boatman, P. D.; Ogbu, C. O.; Eguchi, M.; Kim, H. O.; Nakanishi, H.; Cao, B. L.; Shea, J. P.; Kahn, M. *J. Med. Chem*. **1999**, *42*, 1367.
12. St. Charles, R.; Matthews, J. H.; Zhang, E. L.; Tulinsky, A. *J. Med. Chem*. **1999**, *42*, 1376.
13. Sorimachi, H.; Ishiura, S.; Suzuki, K. *Biochem. J*. **1997**, *328*, 721.
14. Li, Z.; Ortega-Vilain, A. C.; Patil, G. S.; Chu, D. L.; Foreman, J. E.; Eveleth, D. D.; Powers, J. C. *J. Med. Chem*. **1996**, *39*, 4089.
15. Chatterjee, S.; Gu, Z. Q.; Dunn, D.; Tao, M.; Josef, K.; Tripathy, R.; Bihovsky, R.; Senadhi, S. E.; O'Kane, T. M.; McKenna, B. A.; Mallya, S.; Ator, M. A.; Bozyczko-Coyne, D.; Siman, R.; Mallamo, J. P. *J. Med. Chem*. **1998**, *41*, 2663.

16. Chatterjee, S.; Dunn, D.; Tao, M.; Wells, G.; Gu, Z. Q.; Bihovsky, R.; Ator, M. A.; Siman, R.; Mallamo, J. P. *Bioorg. Med. Chem. Lett*. **1999**, *9*, 2371.
17. Earnshaw, W. C.; Martins, L. M.; Kaufmann, S. H. *Annu. Rev. Biochem*. **1999**, *68*, 383.
18. Brady, K. D.; Giegel, D. A.; Grinnell, C.; Lunney, E.; Talanian, R. V.; Wong, W.; Walker, N. *Bioorg. Med. Chem*. **1999**, *7*, 621.
19. Villa, P.; Kaufmann, S. H.; Earnshaw, W. C. *Trends Biochem. Sci*. **1997**, *22*, 388.
20. Rudel, T. *Herz* **1999**, *24*, 236.
21. Krishnan, R.; Tulinsky, A.; Vlasuk, G. P.; Pearson, D.; Vallar, P.; Bergum, P.; Brunck, T. K.; Ripka, W. C. *Protein Sci*. **1996**, *5*, 422.
22. Taylor, M. J.; Hoffman, T. Z.; Yli-Kauhaluoma, J. T.; Lerner, R. A.; Janda, K. D. *J. Am. Chem. Soc*. **1998**, *120*, 12783.
23. Albers, M. W.; Walsh, C. T.; Schreiber, S. L. *J. Org. Chem*. **1990**, *55*, 4984.
24. Taylor, M. J.; Yli-Kauhaluoma, J. T.; Ashley, J. A.; Wirsching, P.; Lerner, R. A.; Janda, K. D. *J. Chem. Soc., Perkin Trans. 1* **1999**, 1133.
25. Karuso, P.; Kessler, H.; Mierke, D. F. *J. Am. Chem. Soc*. **1990**, *112*, 9434.
26. Itoh, S.; DeCenzo, M. T.; Livingston, D. J.; Pearlman, D. A.; Navia, M. A. *Bioorg. Med. Chem. Lett*. **1995**, *5*, 1983.
27. Bach, R. D.; Mintcheva, I.; Kronenberg, W. J.; Schlegel, H. B. *J. Org. Chem*. **1993**, *58*, 6135.
28. Pranata, J.; Jorgensen, W. L. *J. Am. Chem. Soc*. **1991**, *113*, 9483.
29. Hübner, H.; Leeser, A.; Burkert, A.; Ramsay, D. A.; Hüttner, W. *J. Mol. Spectrosc*. **1997**, *184*, 221.
30. Coitino, E. L.; Tomasi, J. *Chem. Phys*. **1996**, *204*, 391.
31. Stanton, J. F.; Gauss, J. *Spectrochim. Acta. A*. **1997**, *53*, 1153.
32. Van Duyne, G. D.; Standaert, R. F.; Karplus, P. A.; Schreiber, S. L.; Clardy, J. *Science* **1991**, *252*, 839.
33. De Maré, G. R. *J. Mol. Struct. (Theochem)* **1992**, *253*, 199.
34. Tyrrell, J. *J. Mol. Struct. (Theochem)* **1992**, *258*, 41.
35. Ottinger, C.; Winkler, T. *Chem. Phys. Lett*. **1999**, *314*, 411.
36. Scuseria, G. E.; Schaefer III, H. F. *J. Am. Chem. Soc*. **1989**, *111*, 7761.
37. Helgaker, T.; Gauss, J.; Jørgensen, P.; Olsen, J. *J. Chem. Phys*. **1997**, *106*, 6430.
38. Goodman, L.; Pophristic, V.; Weinhold, F. *Acc. Chem. Res*. **1999**, *32*, 983.
39. Samdal, S. *J. Mol. Stru*. **1998**, *440*, 165.
40. Sandrone, G.; Dixon, D. A.; Hay, B. P. *J. Phys. Chem. A* **1999**, *103*, 893.
41. Jewett, J. Personal Communication.
42. Fantoni, A. C.; Caminati, W. *J. Chem. Soc., Faraday Trans* **1996**, *92*, 343.
43. Jorgensen, W. L.; Maxwell, D. S.; Tirado-Rives, J. *J. Am. Chem. Soc*. **1996**, *118*, 11225.
44. Rizzo, R. C.; Jorgensen, W. L. *J. Am. Chem. Soc*. **1999**, *121*, 4827.
45. Beak, P.; Lee, J.-K.; Zeigler, J. M. *J. Org. Chem*. **1978**, *43*, 1536.
46. Lamb, M. L.; Jorgensen, W. L. *J. Med. Chem*. **1998**, *41*, 3928.
47. Schaefer III, H. R. *J. Am. Chem. Soc*. **1975**, *97*, 7210.
48. Wiberg, K. B.; Hadad, C. M.; Rablen, P. R.; Cioslowski, J. *J. Am. Chem. Soc*. **1992**, *114*, 8644.
49. Wiberg, K. B.; Rablen, P. R.; Marquez, M. *J. Am. Chem. Soc*. **1992**, *114*, 8654.
50. Saebo, S. *Chem. Phys*. **1987**, *113*, 383.
51. Fogarasi, G.; Lui, R.; Pulay, P. *J. Phys. Chem*. **1993**, *97*, 4036.
52. Schultz, G.; Hargittai, I. *J. Phys. Chem*. **1993**, *97*, 4966.
53. Mack, H. G.; Oberhammer, H. *J. Am. Chem. Soc*. **1997**, *119*, 3567.
54. Samdal, S.; Seip, R. *J. Mol. Struct*. **1997**, *413*, 423.
55. Wiberg, K. B. *Acc. Chem. Res*. **1999**, *32*, 922.
56. Kende, A. S.; Liu, K.; Kaldor, I.; Dorey, G.; Koch, K. *J. Am. Chem. Soc*. **1995**, *117*, 8258.
57. Frisch, M. J.; Trucks, G. W.; Schlegel, H. B.; Scuseria, G. E.; Robb, M. A.; Cheeseman, J. R.; Zakrzewski, V. G.; Montgomery, J. A. J.; Stratmann, R. E.; Burant, J. C.; Dapprich, S.; Millam, J. M.; Daniels, A. D.; Kudin, K. N.; Strain, M. C.; Farkas, O.; Tomasi, J.; Barone, V.; Cossi, M.; Cammi, R.; Mennucci, B.; Pomelli, C.; Adamo, C.; Clifford, S.; Ochterski, J.; Petersson, G. A.; Ayala, P. Y.; Cui, Q.; Morokuma, K.; Malick, D. K.; Rabuck, A. D.; Raghavachari, K.; Foresman, J. B.; Cioslowski, J.; Ortiz, J. V.; Stefanov, B. B.; Liu, G.; Liashenko, A.; Piskorz, P.; Komaromi, I.; Gomperts, R.; Martin, R. L.; Fox, D. J.; Keith, T.; Al-Laham, M. A.; Peng, C. Y.; Nanayakkara, A.; Gonzalez, C.; Challacombe, M.; Gill, P. M. W.; Johnson, B.; Chen, W.; Wong, M. W.; Andres, J. L.; Gonzalez, C.; Head-Gordon, M.; Replogle, E. S.; Pople, J. A. GAUSSIAN 98. Gaussian: Pittsburgh, 1998.
58. Besler, B. H.; Merz, K. M. J.; Kollman, P. A. *J. Comp. Chem*. **1990**, *11*, 431.
59. Bayly, C. I.; Cieplak, P.; Cornell, W. D.; Kollman, P. A. *J. Phys. Chem*. **1993**, *97*, 10269.
60. Jorgensen, W. L. BOSS *Version 4.1*; Yale University: New Haven, CT 1999.
61. Jorgensen, W. L.; McDonald, N. A. *J. Mol. Struct. (Theochem.)* **1998**, *424*, 145.
62. The creation of a new atom type CG required modification and recompilation of the source code for the program BOSS.
63. Boys, S. F.; Bernardi, F. *Mol. Phys*. **1970**, *19*, 553.
64. van Duijneveldt, F. B. In *Molecular Interactions*; Scheiner, S., Ed.; John Wiley & Sons: Chichester, 1997; pp 81–104.